PROCEEDINGS OF SCIENCE

Kr Isotopic Compositions in Stardust SiC grains and AGB Winds

J. Buntain*
Monash Centre for Astrophysics – Monash University, Victoria, Australia
E-mail: Joelene.Buntain@monash.edu
M. Lugaro
Monash Centre for Astrophysics – Monash University, Victoria, Australia
E-mail: Maria.Lugaro@monash.edu
C. Iliadis
Department of Physics & Astronomy – University of North Carolina, North Carolina, USA
E-mail: iliadis@unc.edu
R. Raut
Triangle Universities Nuclear Laboratory – Duke University, North Carolina, USA
E-mail: raut@tunl.duke.edu
A. Tonchev
Triangle Universities Nuclear Laboratory – Duke University, North Carolina, USA
E-mail: tonchev2@llnl.gov
A. I. Karakas
Mount Stromlo Observatory – Australian National University, Canberra, Australia
E-mail: akarakas@mso.anu.edu.au

Krypton (Kr) is a heavy noble gas that does not chemically react and hence does not condense into dust. However, it is found in trace amounts inside stardust silicon carbide (SiC) grains in meteorites, which are believed to have condensed in the C-rich envelopes of low-mass asymptotic giant branch (AGB) stars. The measured isotopic composition of Kr clearly reveals the signature of the *s* (*slow* neutron-capture) process. It is likely that Kr is ionised and implanted in stardust SiC grains via stellar winds in two different evolutionary phases: one during the AGB phase in small grains showing low ^{86}Kr/^{82}Kr, and another during the post-AGB phase in large grains showing high ^{86}Kr/^{82}Kr ratios. The low ^{86}Kr/^{82}Kr ratios observed in stardust SiC grains can be explained by model predictions of AGB winds. On the other hand, to explain the high ^{86}Kr/^{82}Kr ratios we need to look at the material in the winds of the post-AGB phase. We present Kr isotopic compositions predicted by *s*-process AGB-star models of different masses and metallicities, and compare them to data from stardust SiC grains. We find that to match the high ^{86}Kr/^{82}Kr ratios observed in the large grains, a proton ingestion during the thermal pulse (TP) may be required. We also find that the ^{84}Kr(n,γ)^{85}Kr neutron-capture cross section should to be lower than the current estimate in order for our models to match the pure *s*-process value.

XII International Symposium on Nuclei in the Cosmos,
August 5-12, 2012
Cairns, Australia

*Speaker.

PoS(NIC XII)144

1. Introduction

Kr is a heavy noble gas that is chemically inactive and therefore does not condense into dust. However, it has been found in trace amounts in stardust silicon carbide (SiC) grains found in meteorites. The vast majority of these grains are believed to condense in the C-rich envelopes of low-mass asymptotic giant branch (AGB) stars. The isotopic composition of Kr in stardust SiC grains clearly reveals the signature of mixing of pure *s*-process material and solar composition material (Ref. [1]).

The *s* process is responsible for the production of about half of the elements heavier than Fe. It occurs at low neutron densities ($\lesssim 10^8$ n/cm^3) and in the hydrostatic phases of stellar evolution. During the *s* process, stable isotopes capture neutrons. When radioactive isotopes are produced, they generally decay to their stable daughter isotope before capturing a neutron. However, if the neutron density is high enough, also depending on the temperature and density, some unstable nuclei with relatively long half-lives (longer than $\sim$ few days) can capture additional neutrons rather than decay (branching points).

The *s* process occurs in AGB stars, which are the final phases of evolution in low-mass stars ($\lesssim 8M_\odot$). The AGB structure consists of an electron-degenerate C-O core surrounded by H- and He-burning shells that burn alternatively. They are separated by a thin He-intershell with a convective H-rich envelope surrounding them all. The H-burning shell is the site for nuclear energy production. Approximately every 10^5 years the He shell ignites and drives convection throughout most of the He intershell. These instabilities are known as thermal pulses (TPs). After a TP has occurred, the energy released from it causes the whole star to expand and cool. This pushes the H-burning shell outwards, causing it to cool and to be extinguished. The convective envelope can then extend inward, reaching the He intershell. This is known as the third dredge-up (TDU) and mixes nuclear-processed material from the He- and H-burning shells to the stellar surface. The *s* process occurs in the intershell where neutrons are released by the ^{13}C(α,n)^{16}O reaction, which occurs at relatively low temperatures ($\sim 0.9\times10^8$K), such as during the interpulse periods, and results in low neutron densities (10^6-10^7 n/cm^3). The ^{22}Ne(α,n)^{25}Mg reaction is activated only at relatively high temperatures ($\gtrsim$3x10^{8}K), which can occur during TPs in intermediate-mass AGB stars (M>3M$_\odot$ and depending on metallicity) and results in higher neutron densities ($\sim 10^{10}$ n/cm^3).

The amount of ^{86}Kr produced by the *s* process is determined by the branching point at the unstable ^{85}Kr, which has a half-life of 10.76 years. When the *s* process reaches this isotope, two events can occur. If the neutron density remains fairly low then it will decay to ^{85}Rb. However, if the neutron density is high ($\gtrsim 5\times10^8$ n/cm^3), more than 50% of the time ^{85}Kr will capture a neutron and make ^{86}Kr. The other 50% of the time, the ^{85}Kr will decay to ^{85}Rb.

Ref. [2] proposed that Kr was ionised and implanted in stardust SiC grains via stellar winds in two energy components: one during the AGB phase in the small grains with low ^{86}Kr/^{82}Kr ratios, and the other during the post-AGB phase in the large grains with high ^{86}Kr/^{82}Kr ratios. The difference between the two phases is the wind speeds. For the AGB phase the speeds are low (10-30 km/s) while the speed during the post-AGB phase can reach up to a few thousand km/s.

The low ^{86}Kr/^{82}Kr ratios should be explained by model predictions of AGB winds (Ref. [3]). To explain the high ^{86}Kr/^{82}Kr ratios, we need to look at the material in the He intershell at the end of the AGB evolution as this material represents the *s*-process component in the post-AGB winds.

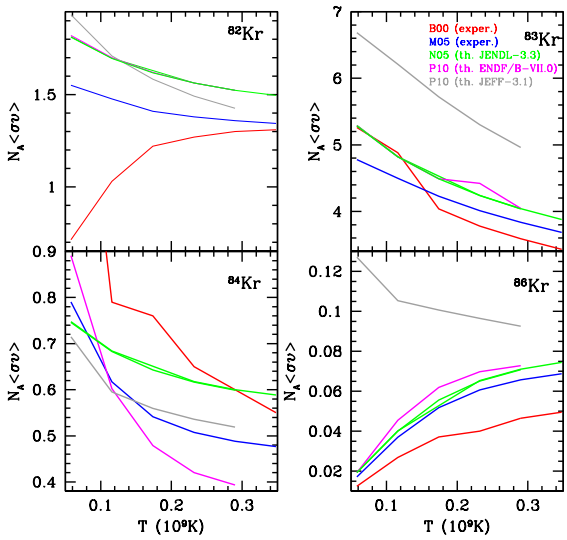

Figure 1: Neutron-capture rates (N_A $<\sigma\ \upsilon>$in $cm^{3-1}mole^{-1}s^{-1}$) of Kr isotopes as a function of temperature. Each line corresponds to either a theoretical (th.) or experimental (exper.) estimate of that cross-section, as determined by the mentioned authors, where B00 = Ref. [7], M05 = Ref. [8], N05 = Ref. [9] and P10 = Ref. [10].

2. Method & Results

For this study we used four stellar evolutionary sequences that become C-rich during the AGB phase: a $1.25M_\odot$ star of metallicity (Z) = 0.01 and a $1.8M_\odot$ star of Z = 0.01 (Ref. [4]), and two $3M_\odot$ stars of Z= 0.01 (Shingles & Karakas 2012, in preparation) and Z = 0.02 (Ref. [5]). A post-processing code with 320 species and 2,336 reactions was used to perform the *s*-process nucleosynthesis calculations. We artifically included some protons in the top layers of the He intershell to allow for the formation of the ^{13}C neutron source as explained in detail in [6]. We used neutron-capture cross sections for the stable Kr isotopes (^{82}Kr, ^{83}Kr, ^{84}Kr, ^{86}Kr) from Refs. [7], [8], [9] and [10], and our new determination of the ^{85}Kr(n,γ)^{86}Kr rate from Raut et al. (in prep.).

Figure 1 shows the neutron-capture rates for Kr isotopes used in our network (N_A $<\sigma\upsilon>$in $cm^3mole^{-1}s^{-1}$) as a function of temperature. From these plots we see that the rates proposed by different authors vary greatly when taken from different authors. A recent measurement of the ^{86}Kr(γ,n)^{85}Kr (Raut et al., in preparation) provides an improved estimate of the ^{85}Kr(n,γ)^{86}Kr reaction rate. A preliminary data analysis hints that this rate is $\sim$20% higher than the current estimate of Ref. [7].

Figure 3 plots ^{83}Kr/^{82}Kr versus ^{84}Kr/^{82}Kr stellar model predictions for pure *s*-process material in the winds during the post-AGB phase, compared to stardust SiC grain data from Ref. [1]. The models represent the pure *s*-process material from the He intershell at the end of the AGB evolution. In order to match the stardust SiC grain measurements the models should sit on the mixing line defined by the grain data, however, the theoretical ratios are clearly off the line. We

estimate the ^{84}Kr/^{82}Kr ratio from the stardust SiC grain data by taking the average of the predicted ^{83}Kr/^{82}Kr ratio, as this ratio does not change significantly. By extrapolating the mixing line defined by the stardust SiC grain data we derived the *s*-process value of the ^{84}Kr/^{82}Kr ratio to be 2.6. The ^{84}Kr(n,γ)^{85}Kr cross sections determined by Refs. [8] and [9] gave results closest to this derived ^{84}Kr/^{82}Kr *s*-process value of 2.6. When we took the 1.8M$_{\odot}$, Z = 0.01 model and lowered the ^{84}Kr(n,γ)^{85}Kr cross section of Ref. [8] by 17%, we found an almost perfect match with the extrapolated ^{84}Kr/^{82}Kr *s*-process value.

Figure 3 shows ^{86}Kr/^{82}Kr versus ^{84}Kr/^{82}Kr isotopic ratios compared to stardust SiC grain data. Most of the models have the low ^{86}Kr/^{82}Kr ratios observed in the small grains. The 1.25M$_{\odot}$, Z = 0.01 model is the closest to matching the high ^{86}Kr/^{82}Kr ratios observed in the large grains. This is because in this model some of the ^{13}C neutron source is ingested during the TP as the temperatures are too low for all of the ^{13}C source to be burnt before the onset of the TP, as also seen in models computed by Ref. [11]. This allows higher neutron densities, favouring more effecient activation of the branching point and leading to a higher production of ^{86}Kr. We experimented with proton ingestion during the last TP of the 1.8M$_{\odot}$, Z=0.01 model where we artificially inserted a small amount of protons (4×10^{-6}M$_{\odot}$) at the top of the TP to produce extra ^{13}C. Proton ingestions are believed to occur in very late thermal pulses (VLTP) when H burning is off [12]. The Pulse-driven convection zone of the He-burning shell can penetrate the H-rich envelope, then protons are ingested into the C-rich intershell region and captured by the reaction ^{12}C(p,γ)^{13}N and protons are are burnt on the way to the interior. The intershell abundances are then exposed at the stellar surface. Since we are not considering a VLTP, our model should be considered as a simple test exercise. Figure 3 shows that the ^{86}Kr/^{82}Kr ratios of this model ("PI") are now closer to matching the large grains.

3. Summary & Future work

Figure 3 shows that if we lower the ^{84}Kr(n,γ)^{85}Kr cross-section from Ref. [8] by 17%, we are able to match the ^{84}Kr/^{82}Kr *s* process value inferred from stardust SiC grain data. Given our new determination of the ^{85}Kr(n,γ)^{86}Kr rate from Raut et al. (in prep.), the high ^{86}Kr/^{82}Kr ratios observedin the large stardust SiC grains can be explained if some of the main ^{13}C neutron source burns convectively during the AGB TP driven by He burning. As shown in Fig. 3, ingestion of ^{13}C during the TP in the 1.25M$_{\odot}$ model allows a closer match to the high ^{86}Kr/^{82}Kr observed in the grains. If we simulate ingestion of 4×10^{-6} M$_{\odot}$ of protons in the final pulse of the 1.8M$_{\odot}$ model, we are also able to achieve these high ratios.

Future work will entail investigating if it is possible for a stronger activation of the ^{22}Ne source in some of the models, which may also lead to the high ^{86}Kr/^{82}Kr ratios observed in large SiC grains. We will also model the production of ^{80}Kr and compare the results to SiC data as well as compare the grain data with model predictions for the other noble gases, He, Ne, Ar and Xe.

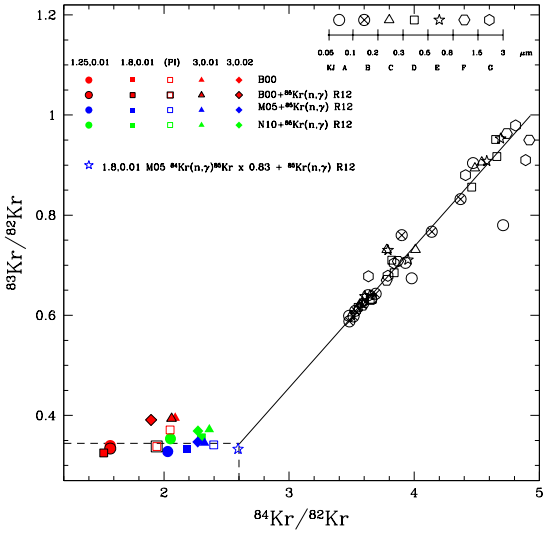

Figure 2: The ^{83}Kr/^{82}Kr versus ^{84}Kr/^{82}Kr isotopic ratios compared to stardust SiC grain data from Ref. [1]. The models are defined by different symbols and different reaction rates are represented by different colours. B00 indicates models run with the neutron-capture cross sections from [7]. B00 + ^{85}Kr(n,γ) R12 refers to models run with the neutron-capture cross sections from [7] with the latest ^{85}(n,γ)^{86}Kr reaction rate from Raut et al. (2012, in preparation). M05 + ^{85}Kr(n,γ) R12 and N10 + ^{85}Kr(n,γ) R12 are models run with the neutron-capture cross sections from [8] and [9], respectively, both using the new estimate for the ^{85}(n,γ)^{86}Kr reaction rate from Raut et al. (2012, in preparation). The different symbols for the grain data represent different grains sizes (Murchison meteorite separates KJA-KFG). The solid black line is the best fit through the stardust SiC grain data and is taken to represent the mixing line that connects pure *s*-process material (lower left) with solar composition material (upper right). The dashed black lines in the lower left corner represent our estimation of the ^{84}Kr *s*-process value. See Fig. 1 for references.

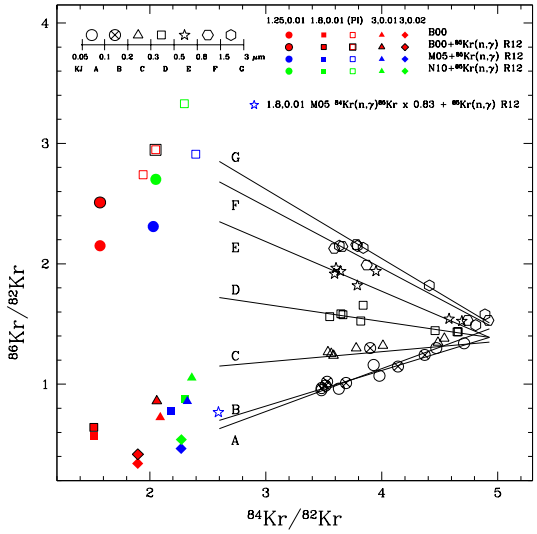

Figure 3: Same as Fig. but for the ^{86}Kr/^{82}Kr versus ^{84}Kr/^{82}Kr isotopic ratios.

References

[1] R. S. Lewis, S. Amari, and E. Anders, *Interstellar grains in meteorites: II. SiC and its noble gases*, *Geochim. Cosmochim. Acta* **58** (Jan., 1994) 471–494.

[2] A. B. Verchovsky, I. P. Wright, and C. T. Pillinger, *Astrophysical Significance of Asymptotic Giant Branch Stellar Wind Energies Recorded in Meteoritic SiC Grains*, *ApJ* **607** (June, 2004) 611–619.

[3] M. Pignatari, R. Gallino, S. Amari, and A. M. Davis, *Krypton in presolar mainstream SiC grains from AGB stars*, *MemSaIt* **77** (2006) 897.

[4] A. I. Karakas, S. W. Campbell, and R. J. Stancliffe, *Is Extra Mixing Really Needed in Asymptotic Giant Branch Stars?*, *ApJ* **713** (Apr., 2010) 374–382.

[5] A. I. Karakas, *Updated stellar yields from asymptotic giant branch models*, *Mon. Not. R. Astron. Soc.* **403** (Apr., 2010) 1413–1425.

[6] M. Lugaro, C. Ugalde, A. I. Karakas, J. Görres, M. Wiescher, J. C. Lattanzio, and R. C. Cannon, *Reaction Rate Uncertainties and the Production of 19F in Asymptotic Giant Branch Stars*, *ApJ* **615** (Nov., 2004) 934–946.

[7] Z. Y. Bao, H. Beer, F. Käppeler, F. Voss, K. Wisshak, and T. Rauscher, *Neutron Cross Sections for Nucleosynthesis Studies*, *Atomic Data and Nuclear Data Tables* **76** (Sept., 2000) 70–154.

[8] P. Mutti, H. Beer, A. Brusegan, F. Corvi, and R. Gallino, *New Kr Cross Sections and Astrophysical Constraints on Presolar Grains*, in *International Conference on Nuclear Data for Science and Technology* (R. C. Haight, M. B. Chadwick, T. Kawano, and P. Talou, eds.), vol. 769 of *American Institute of Physics Conference Series*, pp. 1327–1330, May, 2005.

[9] T. Nakagawa, S. Chiba, T. Hayakawa, and T. Kajino, *Maxwellian-averaged neutron-induced reaction cross sections and astrophysical reaction rates for kT = 1 keV to 1 MeV calculated from microscopic neutron cross section library JENDL-3.3*, *Atomic Data and Nuclear Data Tables* **91** (Nov., 2005) 77–186.

[10] B. Pritychenko, S. F. Mughaghab, and A. A. Sonzogni, *Calculations of Maxwellian-averaged cross sections and astrophysical reaction rates using the ENDF/B-VII.0, JEFF-3.1, JENDL-3.3, and ENDF/B-VI.8 evaluated nuclear reaction data libraries*, *Atomic Data and Nuclear Data Tables* **96** (Nov., 2010) 645–748, [0905.2086].

[11] S. Cristallo, L. Piersanti, O. Straniero, R. Gallino, I. Domínguez, C. Abia, G. Di Rico, M. Quintini, and S. Bisterzo, *Evolution, Nucleosynthesis, and Yields of Low-mass Asymptotic Giant Branch Stars at Different Metallicities. II. The FRUITY Database*, *ApJ* **197** (Dec., 2011) 17.

[12] T. Blöcker, *Evolution on the AGB and beyond: on the formation of H-deficient post-AGB stars*, astro-ph/0102135.